


## RESEARCH ARTICLE

# The Analysis of Liquefaction Potential and Post-Liquefaction Deformations at a Highway Bridge Crossing

Nazife Erarslan<sup>1,\*</sup> and Büşra Şen<sup>1</sup> <sup>1</sup>Geotechnical Department, İzmir Demokrasi University, Türkiye

**Abstract:** The primary goal of this study is to geotechnically analyze the soil strength and liquefaction potential of the soil where the Seyrek highway junction and the bridge are built under earthquake-related dynamic stress. The analyses include comparisons of liquefaction potential using various empirical approaches, studies of post-liquefaction vertical deformation, and investigations into the influence of fill soil on liquefaction-induced surface deformation. Since the analyses of liquefaction potential in soils are made based on the “Simplified Method” approach, this method was also used in this study. This study also used the “Simplified Method” approach, which is the basis for studies of soil liquefaction potential. Four standard penetration tests (SPTs) on the bridge piers were used to collect field data, and experiments in the lab were used to establish the requisite soil parameters. When the results of the Simplified Method analysis were performed according to the soil properties of the SK-1, SK-2, SK-3, and SK-4 drillings and the liquefaction analysis results were determined according to the required safety factor (Fs), liquefaction potential up to 18.5 m was determined in all four SPT locations. Moreover, the results of surface damage effect analyses of the non-liquefied cover/fill layer on the Seyrek crossing bridge soil for all four SPP fields were found to be “visible” and the liquefiable layer thickness (H2) was found to be 10.5 m. The calculated liquefaction severity index (LS) value was found to be up to 52, which means the liquefaction effect was found to be “Possible liquefaction damage”.

**Keywords:** soil liquefaction, liquefaction potential and simplified method, lateral spreading and liquefaction, liquefaction severity indices

## 1. Introduction

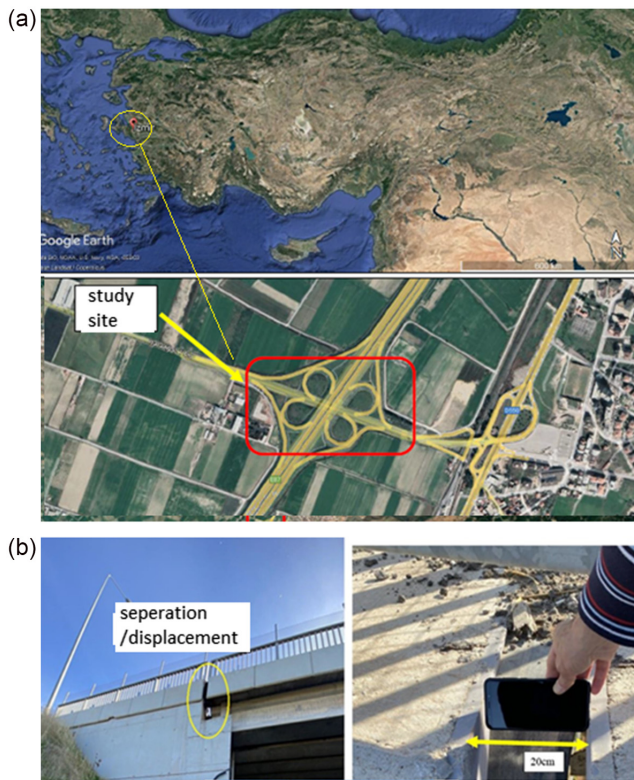
Regional ground conditions significantly impact the damage caused by earthquakes to structures. During an earthquake, different soil types produce seismic waves in different ways, and their effect on structures depends on the properties of the soil. Many earthquakes, such as those in Niigata in 1964 and Kobe in 1995 in Japan, highlighted the impact and possibility of soil liquefaction on the world. Liquefaction is one of the most dramatic events and causes of damage to structures during an earthquake. However, liquefaction does not necessarily occur as a result of any strong earthquake. There are many environmental and soil-related factors that affect the formation of liquefaction. For example, environmental factors such as the focal distance of the earthquake, liquefiable soil layer thicknesses, and groundwater level are important factors. The factors related to the soil structure are the basic factors such as the density of the soil, the fine grain ratio, the degree of water saturation, and plasticity properties. Considering all factors, granular material (e.g. sand) with coarse soil grains has proven to be the soil type that is most susceptible to the liquefaction process. A seismic wave can cause a complete loss of soil shear strength if such granular soil is almost completely or even partially saturated with water. Soil particles begin to move freely in the water and the ground liquefies, acting as a thick layer of liquid.

In this case, liquefaction can be briefly explained as follows: Certain materials tend to reduce volume or compactness during the application of any type of load (static or dynamic). Since earthquake load is a cyclic and rapid type of loading, the soil is not likely to discharge/drain the water in the pores and a sudden increase in pore water pressure develops. With this increase in pore water pressure, the effective stress in the soil decreases. When the pore pressure reaches the value of the total stresses, liquefaction occurs as a result of the loss of stiffness and soil shear strength; liquefaction damage and liquefaction-induced soil settlement occur.

The study area is located in the Menemen district of İzmir province and is approximately 7 km away from the southwest of the center of the district. Transportation to the region can be provided via the Menemen-İzmir highway (Figure 1). Aegean Region in Turkey is a region with high earthquake risk with tens of active faults. There are active fault zones in the west and south of İzmir, extending to North-South and N.NE-S.SW. According to the Turkish Hazard Active Fault Inventory [1], there is the Menemen Fault Zone 12.3 km northeast of the study area. When the drilling data in the study area are examined, the groundwater level varies between 3.10 and 4.05 m. When the drilling data were examined, mostly greenish colored, loose, silty sand containing very little fine gravel, light brown colored, solid, silty clay with very little fine gravel, and light brown-grayish colored very solid silt units were observed in the region. The groundwater level, the earthquake zone, and the presence of sand-silt mixed soil already show that the study area has a high liquefaction potential.

\*Corresponding author: Nazife Erarslan, Geotechnical Department, İzmir Demokrasi University, Türkiye. Email: [nazife.dogan@idu.edu.tr](mailto:nazife.dogan@idu.edu.tr)

**Figure 1**  
**Study site and (b) deformations on Seyrek bridge on highway junction**



In the bridge located at the Seyrek Junction on the Menemen-Aliğa Highway, 10–20 cm segregation deformations due to rotation in the bridge piers and similar deformations in the canal bridge located near it were detected. The main purpose of this study is to examine the deformation characteristics, soil strength against liquefaction, and liquefaction potential under dynamic loads from the geotechnical point of view of the ground where the junction and bridge are built. Seyrek bridge junction and canal bridges are structures built on reclaimed ground by filling method. It is also

aimed to determine whether liquefaction causes the detected deformations and to help determine the most appropriate soil reinforcement method(s) in the “soil reinforcement” research to be applied later to these two previously built structures.

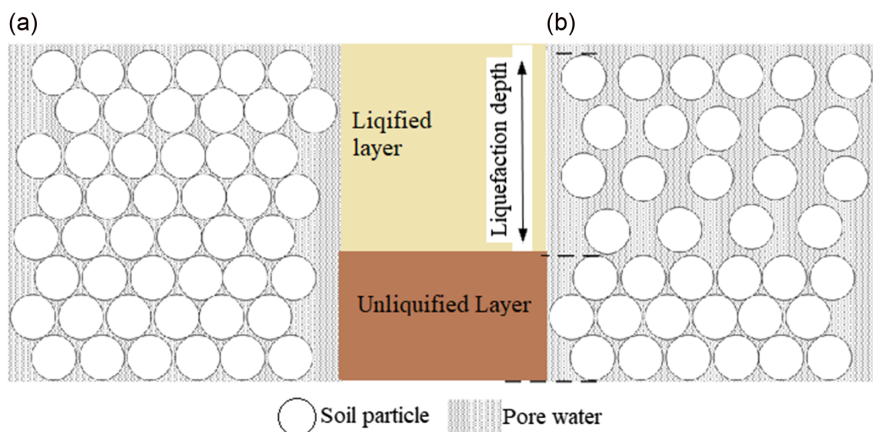
**2. Literature Review**

During dynamic loads such as earthquakes, loose and saturated sand grains break up, and loosely packed soil particles try to shift into a denser configuration. However, in case of earthquake loading, there is not enough time for the pore water of the soil to come out. Instead, water is trapped and prevents soil particles from converging and re-stacking (Figure 2). Therefore, there is an increase in pore water pressure, which reduces the contact forces between individual soil particles, resulting in a loss of strength leading to liquefaction of the soil [2–6].

The term “liquified,” which means “liquefied” in soil mechanics, was first defined by Allen Hazen in 1918 as a result of the collapse of the Calaveras dam in California [7]. Karl Terzaghi, who is accepted as the founder of soil mechanics all over the world, made important research in the field of soil mechanics in Istanbul between 1916 and 1925. One of the most important results of Terzaghi’s research is considered to be revealing the link between effective stress and pore water pressure in soils. The concepts of effective stress and pore water pressure, which were first introduced by Terzaghi in history, have an important place in the basis of the liquefaction mechanism [2, 5, 8–10].

Once a particular soil has been determined to be susceptible to liquefaction on the basis of various susceptibility criteria, the next step in the liquefaction hazard assessment process is the assessment of its liquefaction potential [11]. In recent years, researchers have proposed different methods to understand the liquefaction mechanism and to determine the liquefaction potential of soils. In general, a variety of approaches are used to assess liquefaction potential, including (i) energy-based approaches, (ii) cyclic stress-based approaches, and (iii) cyclic strain-based approaches [2, 6, 11]. The energy-based approach is theoretically well suited for liquefaction potential assessment because the dissipated energy reflects both the cyclic stress and the strain amplitudes. However, energy-based methods are less widely used due to the lack of in situ data for the calibration of these methods [6, 12]. Cyclic strain-based approaches to

**Figure 2**  
**Soil liquefaction mechanism**



assessing the liquefaction potential have shown that the densification of dry sands is effectively affected by cyclic strain rather than cyclic stress. The cyclic strain approach is not widely used because cyclic strain amplitudes cannot be predicted as accurately as cyclic stress amplitudes and cyclic strain-controlled test equipment is not commonly used. It is less available than cyclic stress-controlled test equipment [13–16]. The variation of cyclic stress ratio (CSR) in cyclic stress-based approaches is obtained using liquefaction cycle number,  $N_{liq}$ . In this approach, initial liquefaction is defined as the pore pressure ratio created reaches one or the induced shear stress reaches a significant value, a single shear stress amplitude of 3.75% [17].

Liquefaction can occur at any depth if the hydrodynamic conditions (also caused by earthquakes) are such that the pore water pressure exceeds the vertical load. Thabet et al. [18] found that soil layers 6–23 m deep were responsible for liquefaction in the Kushiro Port area. Naik et al. [16] found that stratified soils with a liquefaction probability of between 2 and 20 were prone to liquefaction from their detailed analysis of the widespread liquefaction reported around the Heunghae basin, the first reported liquefaction case in Korea's modern seismic history, during the 2017 Mw 5.4 Pohang earthquake.

Li et al. [6] reported that liquefied sandy soil in the lower layers at a depth of 16–17 m moved upwards to the upper clay layer, showing that deep liquefaction occurred at a depth of 18–20 m. Such liquefaction events in field studies are rarely found in the literature.

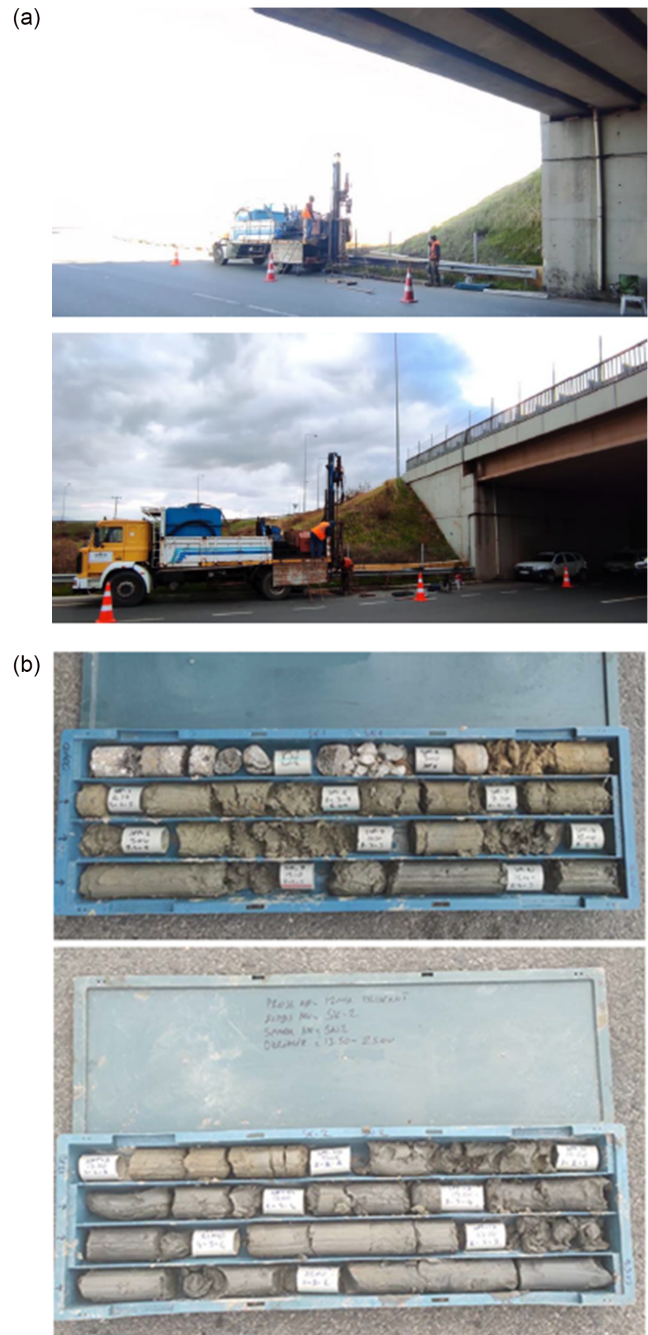
Evaluation of post-liquefaction settlement is important for the analysis of seismic soil behavior. The liquefaction-induced soil settlement of saturated granular soils can be estimated using one of the semi-empirical methods. Such semi-empirical methods are described by Tokimatsu and Seed [19], Ishihara and Yoshimine [20], Shamoto et al. [21], Wu and Seed [22], Cetin et al. [23], and Cetin et al. [24]. Studies have been conducted to correlate liquefaction-induced settlement with shear wave velocity [20, 25, 26].

## 2.1. Theoretical framework and research methodology

The “Simplified Method” analysis, which is one of the most used liquefaction potential and analysis methods, proposed by Seed and Idriss [27] and using standard penetration test (SPT) data, which is one of the in-situ drilling tests, was used in this research (Figure 3). The simplified liquefaction method includes laboratory tests with samples taken from the field such as soil characterization tests and water permeability with SPT data to evaluate the liquefaction potential of the soil.

In the simplified method, parameters such as density, water content, permeability, particle size distribution, and effective normal stress of the samples are measured. By using these parameters, values such as cyclic resistance ratio (CRR), cyclic stress ratio (CSR), and factor of safety (FS) of the soil are calculated. These values are used together in the Simplified Method to indicate the probability of soil liquefaction. Generally, the potential of soil liquefaction is considered low if the FS value is greater than 1.3. This method is redescribed by Youd et al. [28] and updated. In the soil liquefaction literature, the seismic demand (loading) on the soil is simplified and expressed as CSR. On the other hand, the capacity of the soil to resist liquefaction is defined as the CRR [27–29]. The mean cyclic shear stress,  $\tau_{av}$ , developed due to shear waves propagating vertically on the horizontal surface of the soil

Figure 3  
(a) SPT drilling and (b) cored specimens



layers is defined as the inclusion of the increase in shear strength by normalizing the initial effective vertical stress  $\sigma'_v$ . With an increase in effective stress, CSR is found as [28]:

$$CSR = \tau_{av} \frac{\tau_{av}}{\sigma'_v} = 0.65 \frac{\sigma_{max} \sigma'_v}{g \sigma'_v} r_d \quad (1)$$

where  $\sigma'_v$  is the total vertical stress of the soil at the working depth,  $a_{max}$  is the peak horizontal ground surface acceleration,  $g$  is the gravitational acceleration, and  $r_d$  is the shear stress reduction factor.



To evaluate the effect of fine grain content (FC) in soil, Youd et al. [28] introduced the corrected SPT numbers for clean sands and proposed the following formula:

$$CRR_{7.5} = \frac{1}{24 - N_{1.60cs}} + \frac{N_{1.60cs}}{135} + \frac{50}{(10N_{1.60cs} + 45)^2} - \frac{1}{200} \quad (2)$$

where  $N_{1.60cs}$  is the corrected SPT test impact number for sands and is expressed as:

$$N_{1.60cs} = a + bN_{160} \quad (3)$$

$N_{1.60}$  is expressed as the number of corrected SPT impact numbers, and  $a$  and  $b$  are two constant parameters used to account for the effect of fines content FC and both are functions of FC. The coefficients  $a$  and  $b$  are given in Table 1.

**Table 1**  
Effect of fine content on liquefaction parameters

$a = 0$	FC ≤ %5
$a = (1.76 - 190/FC^2)$	%5 < FC < %35
$a = 5$	FC ≥ %35
$b = 1$	FC ≤ %5
$b = 0.99 + FC^{1.5}/1000$	%5 < FC < %35
$b = 1.2$	FC ≥ %35

One measure of the liquefaction potential of the soil is the FS, conceptually defined as the FS = CRR/CSR. Therefore, it is said that the soil is liquefied if FS ≤ 1, and not liquefied if FS > 1 [27]. For safety factor against liquefaction, Youd et al. [28] suggested the following formula:

$$FS = \left( \frac{CRR_{7.5}}{CSR} \right) * MSF * K_{\sigma} * K_{\alpha} \quad (5)$$

where FS is the safety factor against liquefaction;  $CRR_{7.5}$  is the cyclic resistance ratio for earthquakes of equivalent magnitude 7.5; CSR is the cyclic stress ratio for a given quantity; MSF is the magnitude scaling factor;  $K_{\sigma}$  is the overload correction factor; and  $K_{\alpha}$  is the correction factor for sloping ground, assumed equal to 1 for flat ground surface.

For earthquakes of different magnitudes, the scale factor needs to be converted to a scale of 7.5. Seed and Idriss [30] developed an MSF transformation formula that takes into account the appropriateness of calculating a particular earthquake factor:

$$MSF = -0.058 + 6.9 \exp - \left( \frac{M_w}{4} \right) \leq 1.8 \quad (6)$$

Here,  $M_w$  refers to the earthquake moment magnitude to be calculated.

### 3. Results and Discussion

According to the calculations made in Turkey's Disaster and Emergency (AFAD) Turkey Earthquake Hazard Maps Interactive Web Application, the effective ground acceleration of the study area was found to be  $A_o = SDS \times 0.4 = 0.44$ .

Based on the analyses made, the possible causes of the deformations in the bridged junction are considered as the

potential for liquefaction in the loose granular units in the soil profile and consolidation settlement of the clay units. The results of this study include liquefaction potential analyses and post-liquefaction-related settlement analyses, which are among the causes of deformations in the Seyrek bridge junction and lateral spreading analysis. Simplified Method analysis results based on soil properties obtained from SPT drilling data and laboratory tests of SK-1, SK-2, SK-3, and SK-4 and liquefaction analysis results determined according to calculated safety coefficients showed that liquefaction of up to 18.5 m is expected in the SK-1 location soil. According to the SK-2 well data, it was found that up to 13.5 m of liquefaction is expected in the ground. In the analyses made with the SK-3 and SK-4 data, it was determined that up to 18 m of liquefaction is expected in the ground.

In the literature, liquefaction potential is determined at depths up to 10–15 m, which is generally accepted as the maximum liquefaction depth. General assumptions are inevitable in the literature and scientific studies, and ideally, the depth limits of soil liquefaction can be determined. The following question should be asked here: how to determine the depth of the deep liquefied soil beneath if there is no evidence of sand eruption. The most widely used liquefaction assessment methods are known to be based on test data on "liquefied" layers. In the literature, 15 m is generally accepted as the highest depth of liquefaction in soil containing sand. However, the literature has reported liquefaction at depths of 20 m or even deeper [6, 31, 32]. For example, the depth limit in the Chinese seismic design code is 20 m [6]. Evaluation of the Seyrek interchange ground, which is considered in this thesis, concluded that liquefaction analysis of SK-1, SK-3, and SK-4 wells is expected to liquefy up to 20 m.

In accordance with the analysis of Ishihara and Yoshimine [20], the results of the analysis for the SK-1 area are given in Table 2. The amount of lateral spreading after liquefaction, LDI, in the investigated area was found to be 7.38 m. Due to the volumetric unit deformation, the amount of vertical settlement due to reconsolidation after liquefaction was found to be 0.78 m. On the other hand, according to the model proposed by Tokimatsu and Seed [19], the amount of dynamic settlement due to volumetric unit deformation was found to be 0.58 m. According to the analysis results of Ishihara and Yoshimine [20] for the SK-2 well, the amount of lateral displacement after liquefaction, LDI, was found to be 5.13 m. Depending on the volumetric unit deformation, the total amount of settlement in the vertical direction was found to be 0.47 m (Table 3). On the other hand, the vertical settlement amount suggested by Tokimatsu and Seed [19] was found to be 0.33 m. The analysis results for the SK-3 well showed the amount of lateral displacement, LDI, after liquefaction in the investigated area was found to be 7.38 m. Depending on the volumetric unit deformation, the total amount of settlement in the vertical direction was found to be 0.72 m. On the other hand, according to the model proposed by Tokimatsu and Seed [19], the vertical settlement amount was found to be 0.51 m. Finally, the LDI after liquefaction in the investigated area was found to be 7.38 m, and the total amount of settlement was found to be 0.73 m; according to the model proposed by Tokimatsu and Seed [19], on the other hand, the vertical settlement amount was found to be 0.53 m.

Since the non-liquefiable layer (H1) is an important factor for the liquefaction-induced ground surface damage and liquefaction severity index (LS), H1 was used as the key parameter in designing the chart proposed by Sönmez and Gökçeoğlu [33] and given in Figure 4. The areas bounded by the dashed lines in Figure 4 represent three zones:

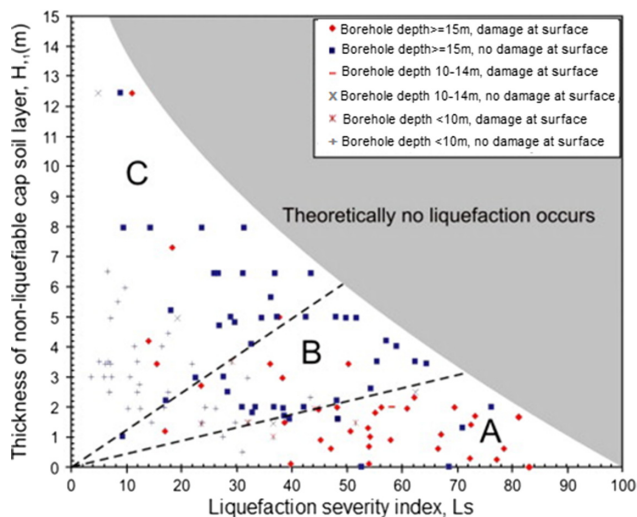
**Table 2**  
**Estimation of vertical and lateral displacement due to liquefaction for SK-1**

Max. shear unit deformation, $g_{max}$	Ishihara and Yoshimine [20]				Tokimatsu and Seed [19]		
	Liquefied soil layer thickness, $\Delta H_i$ (m)	Lateral displacement $\Delta LDI_i$ (m)	Volumetric unit deformation $\epsilon_v$ (%)	Dynamic settlement, $\Delta S_i$ (m)	$CSR_{M,7.5}$	$\epsilon$ (%)	$\Delta H$ (m)
0.5	2.0	1.000	0.041	0.081	0.12	0.028	0.06
0.5	1.5	0.750	0.055	0.083	0.12	0.041	0.06
0.5	1.5	0.750	0.045	0.068	0.13	0.031	0.05
0.5	1.5	0.750	0.046	0.070	0.14	0.032	0.05
0.5	1.5	0.750	0.054	0.081	0.13	0.039	0.06
0.5	2.25	1.125	0.063	0.142	0.13	0.052	0.12
0.5	2.25	1.125	0.060	0.136	0.12	0.048	0.11
0.5	2.25	1.125	0.054	0.122	0.12	0.040	0.09
	<b>LDI = 7.38 m</b>		<b><math>\Sigma S = 0.78</math> m</b>		<b><math>\Sigma S = 0.58</math> m</b>		

**Table 3**  
**Estimation of vertical and lateral displacement due to liquefaction for SK-2**

Max. shear unit Deformation, $g_{max}$	Ishihara and Yoshimine, [20]				Tokimatsu and Seed [19]		
	Liquefied soil layer Thickness, $\Delta H_i$ (m)	Lateral displacement $\Delta LDI_i$ (m)	Volumetric unit Deformation $\epsilon_v$ (%)	Dynamic settlement, $\Delta S_i$ (m)	$CSR_{M,7.5}$	$\epsilon$ (%)	$\Delta H$ (m)
0.5	2.0	1.000	0.058	0.117	0.120	0.045	0.09
0.5	1.5	0.750	0.048	0.072	0.129	0.033	0.05
0.5	1.5	0.750	0.042	0.064	0.135	0.029	0.04
0.5	1.5	0.750	0.044	0.066	0.136	0.030	0.04
0.5	1.5	0.750	0.039	0.058	0.134	0.026	0.04
0.5	2.2	1.125	0.042	0.093	0.131	0.028	0.06
0.01	0.0	0.000	0.006	0.000	0.123	0.023	0.00
0.01	0.0	0.000	0.005	0.000	0.118	—	0.00
	<b>LDI = 5.13 m</b>		<b><math>\Sigma S = 0.47</math> m</b>		<b><math>\Sigma S = 0.33</math> m</b>		

**Figure 4**  
**Liquefaction severity index, thickness of non-liquefiable cap soil, and occurrence of liquefaction-induced surface disruption relationships [33]**



(A) except 25% of the sites, traces of liquefaction are observed, and (B) 75% and (C) 90% of the sites, traces of liquefaction on the ground are not observed [33]. When the FS against liquefaction of a soil profile, which is overlain by a cap soil and is taken place within the zone between the surface and a depth of 20 m, equals unity, it will form a boundary for the zone shown by grey tone in Figure 4. This zone is called as “zone where liquefaction is not theoretically expected” [33].

The post-liquefaction surface damage effect of the non-liquefied fill soil layer on the Seyrek crossing bridge soil was also analyzed. Analyses were made using Ishihara [34] and Sönmez et al. [35] approaches to make comparative analyses. The results of the SK-1 area are given in Table 4. According to the analysis of Ishihara [34], the thickness of the non-liquefied fill soil ( $H_1$ ) is 4.5 m and the thickness of the liquefiable sand soil,  $H_2$  (m), is 14.8 m. The visibility of the liquefaction effect as damage on the surface was found at the “Possible” level (Table 4). Analyses made according to the Sönmez and Gökçeoğlu [33]’s method showed the LS value was to be 54, and the liquefaction effect was found to be “Possible liquefaction damage” (Table 4). The same analyses were performed for SK-2, SK-3, and SK-4. According to the results, the thickness of the liquefiable sandy layer ( $H_2$ ) in the SK-2 well was 10.3 m and the visibility of the liquefaction effect

**Table 4**  
**Effect of overburden/fill soil on liquefaction deformation**

Ishihara (1985)		Sönmez and Gökçeoğlu (2005)	
Liquefiable sand thickness, $H_2$ (m)	Overburden/fill soil thickness, $H_1$ (m)	Liquefaction severity index, $L_s$	
-	4,5	54	
2,00	$a_{maks} = 0.4 \times S_{DS}$	0,18 g	
1,50			
1,50	Visibility of the liquefaction effect on the surface [Chart No:1]	Surface damage condition, [Chart No:2]	
2,25			
1,50			
1,50			
-	$\Sigma H_2=14,8m$	Possible	Possible liquefaction damage

**Chart No:1**

**Chart No:2**

as damage on the surface was found at the level of “Visible”. The  $L_s$  value is 47 and the liquefaction effect was found to be “Possible liquefaction damage.” In the SK-3 well, the liquefiable sandy layer thickness ( $H_2$ ) was 14.8 m and the liquefaction effect in the SK-3 well was found to be “Visible” on the surface. The  $L_s$  value was found to be 51 and the liquefaction effect was found to be “Possible liquefaction damage.” Finally, the thickness of the liquefiable sandy layer ( $H_2$ ) in the SK-4 was 14.8 m, and the visibility of the liquefaction effect as damage to the surface was found at the level of “Visible”. The  $L_s$  value is 53 and the liquefaction effect was found to be “Possible liquefaction damage.”

**4. Conclusion**

The effective ground acceleration of the Seyrek crossing bridge, which is in the study area, was determined as  $A_0 = SDS \times 0.4 = 0.44$ . Based on the Turkey Earthquake Hazard Map, the local soil class of the study area was determined to be ZE. It has been determined that the underground water level varies in the range of 3.10–4.05 m. When the results of the Simplified Method analysis were performed according to the soil properties of the SK-1, SK-2, SK-3, and SK-4 drillings and the liquefaction analysis results were determined according to the required safety factor ( $F_s$ ), liquefaction potential up to 18.5 m was determined in the SK-1 location. According to the SK-2 data, the liquefaction potential of up to 13.5 m in the soil was calculated. In the analyses made with the SK-3 and SK-4 data, liquefaction potential up to 18 m in the soil was determined.

The surface damage effect of the non-liquefied cover/fill layer on the Seyrek crossing bridge soil was found to be “visible.” In addition, the liquefiable layer thickness ( $H_2$ ) was found to be 10.5 m. The liquefaction severity index ( $L_s$ ) value was found to be 54, and the liquefaction effect was found to be “Possible liquefaction damage.” According to the results, the  $H_2$  for SK-2 was found to be 11.5 m

and the visibility of the liquefaction effect as damage to the surface was found at “Possible” level. The  $L_s$  value was found to be 47 and the liquefaction effect was found as “Surface damage condition: “Possible liquefaction damage.” In SK-3,  $H_2$  was found to be 13.4 m, and the visibility of the liquefaction effect as damage on the surface was found at the level of “Possible.” The  $L_s$  value is 51, and the liquefaction effect was found to be “Possible liquefaction damage.” Finally, the  $H_2$  value of SK-4 was found to be 9.75 m, and the visibility of the liquefaction effect as surface damage was found to be “Possible” level. The  $L_s$  value is 53, and the liquefaction effect was found to be “Possible liquefaction damage.”

**Recommendations**

Different methods such as NCEER (National Center for Earthquake Engineering Research), AIJ (Architecture Institute of Japanese), NCREE (National Center for Research on Earthquake Engineering), and HBF (hyperbolic function) methods should be used to determine the liquefaction potential in addition to the “Simplified Method” approach used in this study.

In addition, some recent advanced technologies that assess the underground water potential such as Derdour et al. [36] could be used to strengthen the liquefaction risk studies in soils.

**Acknowledgments**

This study was carried out with the support of İzmir 2nd Regional Directorate of Highways, R&D Unit.

**Ethical Statement**

This study does not contain any studies with human or animal subjects performed by any of the authors.

## Conflicts of Interest

The authors declare that they have no conflicts of interest to this work.

## Data Availability Statement

Data available on request from the corresponding author upon reasonable request.

## Author Contribution Statement

**Nazife Erarslan:** Conceptualization, Methodology, Software, Validation, Formal analysis, Resources, Data curation, Writing – review & editing, Visualization, Supervision, Project administration.  
**Büşra Şen:** Investigation, Writing – original draft.

## References

- [1] Emre, Ö. (2005). Türkiye Diri Fay Haritasının Güncellenmesinde Yeni Yaklaşım ve İlkeler (in Turkish). In *Aktif Tektonik Araştırma Grubu 9. Toplantısı* (in Turkish), 51.
- [2] Beyaz, T., & Sonmezer, Y. B. (2021). Investigation of the effect of the relative density and shear strain on liquefaction of sands. *Pamukkale University, Engineering Science Journal*, 27(3), 431–440.
- [3] Das, B. M. (1983). *Advanced soil mechanics*. USA & UK: Hemisphere Publishing Corporation.
- [4] Güler, E., Savaş, H., & Afacan K. B. (2021) Effect of permeability on liquefaction potential of silty sands. *Arabian Journal of Geosciences*, 14(1410), 2–9, <https://doi.org/10.1007/s12517-021-07822-9>
- [5] Kramer, S. L. (2003). *Geotechnical earthquake engineering*. UK: Pearson Education Limited.
- [6] Li, P., Tian, Z., Bo, J., Zhu, S., & Li Y. (2022). Study on sand liquefaction induced by Songyuan earthquake with a magnitude of M5.7 in China. *Scientific Reports*, 12(1), 9588.
- [7] Hazen, A. (1919). Hydraulic-fill dams. *Transactions of the American Society of Civil Engineers*, 83(1), 1713–1745.
- [8] Bao, X., Jin, Z., Cui, H., Chen, X., & Xie, X. (2019). Soil liquefaction mitigation in geotechnical engineering: An overview of recently developed methods. *Soil Dynamics and Earthquake Engineering*, 120, 273–291.
- [9] Das, B. M. (2008). *Advanced soil mechanics*, 3rd edition. USA: Taylor & Francis.
- [10] Manav, Y., Toprak, S., İnel, M., & Karakaplan, E. (2019). Soil improvement to counter liquefaction using colloidal silica grout injection. *Journal of Environmental Protection and Ecology*, 20(1), 135–145.
- [11] Kramer, S. L. (1996). *Geotechnical earthquake engineering*. USA: Prentice-Hall.
- [12] Dief, H. M., & Figueroa, J. L. (2007). Liquefaction assessment by the unit energy concept through centrifuge and torsional shear tests. *Canadian Geotechnical Journal*, 44(11), 1286–1297.
- [13] Dobry, R., & Abdoun, T. (2015). Cyclic shear strain needed for liquefaction triggering and assessment of overburden pressure factor  $k_\sigma$ . *Journal of Geotechnical and Geoenvironmental Engineering*, 141(11), 24–38.
- [14] Elgamal, A., Yang, Z., Parra, E., & Ragheb, A. (2003). Modeling of cyclic mobility in saturated cohesionless soils. *International Journal of Plasticity*, 19(6), 883–905.
- [15] Kokusho, T., Ito, F., Nagao, Y., & Green, A. R. (2014). Influence of non/low-plastic fines and associated aging effects on liquefaction resistance. *Journal of Geotechnical and Geoenvironmental Engineering*, 138(6), 747–756.
- [16] Naik, S. P., Gwon, O., Park, K., & Kim, Y. S. (2020). Land damage mapping and liquefaction potential analysis of soils from the epicentral region of 2017 Pohang Mw 5.4 Earthquake, South Korea. *Sustainability*, 12(3), 1234.
- [17] Seed, H. B., & Lee, K. L. (1966) Liquefaction of saturated sands during cyclic loading. *Journal of the Soil Mechanics and Foundations Division*, 92(6), 105–134.
- [18] Thabet, M., Nemoto, H., & Nakagawa, K. (2008). Variation process in stiffness inferred by nonlinear inversion during mainshocks at Kushiro Port vertical array site. *Earth, Planets and Space*, 60, 581–589.
- [19] Tokimatsu, K., & Seed, H. B. (1987). Evaluation of settlements in sands due to earthquake shaking. *Journal of Geotechnical Engineering*, 113(8), 861–878.
- [20] Ishihara, K., & Yoshimine, M. (1992). Evaluation of settlements in sand deposits following liquefaction during earthquakes. *Soils and Foundations*, 32(1), 173–188.
- [21] Shamoto, Y., Zhang, J. M., & Tokimatsu, K. (1998). New charts for predicting large residual post-liquefaction ground deformations. *Soil Dynamics and Earthquake Engineering*, 17(7–8), 427–438.
- [22] Wu, J., & Seed, R. B. (2004). Estimating of liquefaction-induced ground settlement (Case studies). In *Proceedings of the Fifth International Conference on Case Histories in Geotechnical Engineering*.
- [23] Cetin, K. O., Bilge, H. T., Wu, J., Kammerer, A. M., & Seed, R. B. (2009a). Probabilistic models for cyclic straining of saturated clean sands. *Journal of Geotechnics and Geoenvironmental Engineering*, 135(3), 371–386.
- [24] Cetin, K. O., Bilge, H. T., Wu, J., Kammerer, A. M., & Seed, R. B. (2009b). Probabilistic model for the assessment of cyclically-induced reconsolidation (volumetric) settlements. *Journal of Geotechnics and Geoenvironmental Engineering*, 135(3), 387–398.
- [25] Vaid, Y. P., & Sivathayalan, S. (2000). Fundamental factors affecting liquefaction susceptibility of sands. *Canadian Geotechnical Journal*, 37(3), 592–606.
- [26] Yoshimine, M., Nishizaki H., Amano, K., & Hosono, Y. (2005). Flow deformation of liquefied sand under constant shear load and its application to analysis of flow slide of the infinite slope. *Soil Dynamics and Earthquake Engineering*, 26(2), 253–264.
- [27] Seed, H. B., & Idriss I. M. (1971). Simplified procedure for evaluating soil liquefaction potential. *Journal of the Soil Mechanics and Foundations Division*, 97(9), 1249–1273.
- [28] Youd, T. L., Idriss, I. M., Andrus, R. D., Arango, I., Castro, G., Christian, J. T., ..., & Stokoe, K. H. (2001). Liquefaction resistance of soils: Summary report from the 1996 NCEER and 1998 NCEER/NSF workshops on evaluation of liquefaction resistance of soils. *Journal of Geotechnical and Geoenvironmental Engineering*, 127(10).
- [29] Hakam, A. (2016). Laboratory liquefaction test of sand based on grain size and relative density. *Journal of Engineering and Technological Sciences*, 48(3), 334–344.
- [30] Seed, H. B., Idriss, I. M., & Arango, I. (1983). Evaluation of liquefaction potential using field performance data. *Journal of Geotechnical Engineering*, 109(3), 458–482.

- [31] Stewart, D., & Knox, R. (1995). What is the maximum depth liquefaction can occur? In *Proceedings of 3rd International Conferences on Recent Advances in Geotechnical Earthquake Engineering and Soil Dynamics*.
- [32] Yang, Y., Chen, L., Sun, R., Chen, Y., & Wang, W. (2017). A depth-consistent SPT-based empirical equation for evaluating sand liquefaction. *Engineering Geology*, 221, 41–49.
- [33] Sönmez, H., & Gökçeoğlu, C. (2005). A liquefaction severity index suggested for engineering practice. *Environmental Geology*, 48, 81–91.
- [34] Ishihara, K. (1985). Stability of natural deposits during earthquakes. In *Proceedings of 11th International Conference on Soil Mechanics and Foundation Engineering*, 321–376.
- [35] Sönmez, B., Ulusay, R., & Sönmez, H. (2008) A study on the identification of liquefaction-induced failures on ground surface based on the data from the 1999 Kocaeli and Chi-Chi earthquakes. *Engineering Geology*, 97(3–4), 112–125.
- [36] Derdour, A., Benkaddour, Y., & Bendahou, B (2022). Application of remote sensing and GIS to assess groundwater potential in the transboundary watershed of the Chott-El-Gharbi (Algerian– Moroccan border). *Applied Water Science*, 12, 136.

**How to Cite:** Erarslan, N. & Şen, B. (2023). The Analysis of Liquefaction Potential and Post-Liquefaction Deformations at a Highway Bridge Crossing. *Archives of Advanced Engineering Science* <https://doi.org/10.47852/bonviewAAES32021376>